Northumbria Research Link

www.northumbria.ac.uk/nrl

northumbria
UNIVERSITY NEWCASTLE

Hygro-thermal effects on vibration and **thermal** buckling behaviours of **functionally graded** beams

Trung-Kien Nguyen[a,*], Ba-Duy Nguyen[a,b], Thuc P. Vo[d], Huu-Tai Thai[e]

[a]*Faculty of Civil Engineering, Ho Chi Minh City University of Technology and Education, 1 Vo Van Ngan Street, Thu Duc District, Ho Chi Minh City, Viet Nam*
[b]*Faculty of Civil Engineering, Thu Dau Mot University, 6 Tran Van On Street, Phu Hoa District, Thu Dau Mot City, Binh Duong Province, Viet Nam*
[c]*Faculty of Engineering and Environment, Northumbria University, Ellison Place, Newcastle upon Tyne, NE1 8ST, UK.*
[d]*School of Engineering and Mathematical Sciences, La Trobe University, Bundoora, VIC 3086, Australia*

Abstract

The hygro-thermal effects on vibration and buckling analysis of **functionally graded** beams are presented in this paper. The present work is based on a higher-order shear deformation theory which accounts for a hyperbolic distribution of transverse shear stress and higher-order variation of in-plane and out-of-plane displacements. Equations of motion are obtained from Lagrange's equations. Ritz solution method is used to solve problems with different boundary conditions. Numerical results for natural frequencies and critical buckling temperatures of **functionally graded** beams are compared with those obtained from previous works. Effects of power-law index, span-to-depth ratio, transverse normal strain, temperature and moisture changes on the results are discussed.

Keywords: Advanced composite beams; Hygro-thermal loadings; Buckling; Vibration.

1. Introduction

Hygro-thermal stresses arising from a variation of temperature and moisture content can affect structural responses of engineering structures. Therefore, an accurate evaluation of environmental exposure is important to investigate hygro-thermal effects on their behaviours. Owing to the low density and high stiffness and strength, composite structures become popular in several applications of aerospace, automotive engineering, construction, etc. They became more attractive due to an introduction of functionally graded (FG) materials. The general benefit of these structures compared to conventional ones is a continuous variation of hygro-thermo-elastic properties in a required direction so that interfacial issues found in laminated composite structures could be neglected.

---

[*]Corresponding author, tel.: +848 3897 2092
   Email address: `kiennt@hcmute.edu.vn` (Trung-Kien Nguyen)

In order to accurately predict hygro-thermo-mechanical behaviours of FG nanobeams and FG plates/beams, several models and approaches have been developed in recent years. Ebrahimi and Salari [1, 2] investigated nonlocal thermo-mechanical buckling and free vibration of FG nanobeams in thermal environments. Ebrahimi and Barati [3] proposed a unified formulation for dynamic analysis of nonlocal heterogeneous nanobeams in hygro-thermal environment. **Zidi et al. [4] analyzed static responses of FG plates under hygro-thermo-mechanical loading using a four variable refined plate theory. Zenkour et al. [5, 6] investigated hygro-thermo-mechanical effects on behaviours of FG plates on elastic foundations. Fazzolari and Carrera [7] studied thermal stability of FG sandwich plates under various through-the-thickness temperature distributions**. Vibration and buckling analysis of FG beams under mechanical loads have been investigated by many authors based on classical beam theory (CBT) ([8, 9]), first-order shear deformation beam theory (FSBT) ([10–14]), higher-order shear deformation beam theory (HSBT)([15–27]). For thermal environments, the thermal stability and vibration analysis of FG beams have studied by many authors with different methods. Esfahani et al. [28] studied nonlinear thermal buckling of FG beams. The nonlinear thermal dynamic buckling of FG beams is also investigated by Ghiasian et al. [29]. Ma and Lee [30] proposed exact solutions for nonlinear bending behaviour of FG beams under an in-plane thermal loading. Malekzadeh and Monajjemzadeh [31] investigated the dynamic thermal response of FG beams under a moving load. Sankar [32] studied the thermal stresses of simply supported FG beams. Wattanasakulpong et al. [33] employed the HSBT to study the buckling and vibration of FG beams under the uniform thermal loading. Sun et al. [34] investigated thermal buckling and post-buckling of FG beams on nonlinear elastic foundation. Trinh et al. [35] used Levy-type solution for studying thermo-mechanical responses of FG beams. Bhangale and Ganesan [36] analyzed thermoelastic buckling and vibration behaviours of FG sandwich beam with constrained viscoelastic core. By using differential quadrature method, Pradhan and Murmu [37] analyzed thermo-mechanical vibration of FG sandwich beams. However, a limited number of researches has been considered to investigate responses of FG beams in moisture environments. Shen [38, 39] studied nonlinear analysis of composite laminated beams in hygro-thermal environments. **Moreover, it is known that Ritz method is efficient to deal with composite and FG beams with arbitrary boundary conditions. The accuracy and efficiency of this approach can be found in some representative earlier works [24, 26, 40–44].**

The objective of this paper is to present hygro-thermal responses of FG beams using a higher-order shear deformation theory in which a higher-order variation of both in-plane and out-of-plane displacement is taken into account. FG beams are composed of ceramic and metal mixtures, and the

material properties are varied according to power-law form. Ritz solution is developed for different boundary conditions to verify the accuracy of the present theory and to investigate the effects of power-law index, span-to-depth ratio, temperature and moisture content on the vibration and buckling responses of FG beams under hygro-thermal loadings.

2. Theoretical formulation

2.1. Material properties

A FG beam made of a mixture of ceramic and metal isotropic materials, which is embedded in a moisture and temperature environment, with length L and uniform section $b \times h$ is considered as shown in Fig. 1. The material properties are varied according to power-law form:

$$P(z) = (P_c - P_m)\left(\frac{2z + h}{2h}\right)^p + P_m \tag{1}$$

where p is the power-law index and P_c and P_m are Young's modulus E, mass density ρ, coefficient of thermal expansion α, coefficient of moisture expansion β, thermal conductivity coefficient k of ceramic and metal materials, respectively.

Moreover, the thermo-elastic material properties of FG beams are also expressed in terms of temperature $T(K)$ ([31]):

$$P(T, z) = H_0(H_{-1}T^{-1} + 1 + H_1T + H_2T^2 + H_3T^3) \tag{2}$$

where H_0, H_1, H_2, H_3 are temperature dependent coefficients for various types of materials (Table 1). It should be noted that both temperature dependency (TD) and temperature independency (TID) are considered in this paper.

2.2. Moisture and temperature distribution

Three different moisture and temperature distributions through the beam depth are considered: uniform moisture and temperature rise, linear moisture and temperature rise and nonlinear moisture and temperature rise.

- Uniform moisture and temperature rise: the temperature and moisture are supposed to be uniform in the beam and increased from a reference T_0 and C_0, thus their current values of temperature and moisture are:

$$T = T_0 + \Delta T \tag{3a}$$

$$C = C_0 + \Delta C \tag{3b}$$

where T_0 and C_0 are reference temperature and moisture, respectively, which are supposed to be at the bottom surface of the beam.

- Linear moisture and temperature rise: the temperature and moisture are linearly increased as follows:

$$T(z) = (T_t - T_b)\left(\frac{2z+h}{2h}\right) + T_b \tag{4a}$$

$$C(z) = (C_t - C_b)\left(\frac{2z+h}{2h}\right) + C_b \tag{4b}$$

where T_t and T_b are temperatures as well as C_t and C_b are moisture content at the top and bottom surfaces of the beam.

- Nonlinear moisture and temperature rise: the temperature and moisture are varied nonlinearly according to a sinusoidal law ([7]) as follows:

$$T(z) = (T_t - T_b)\left[1 - \cos\frac{\pi}{2}\left(\frac{2z+h}{2h}\right)\right] + T_b \tag{5a}$$

$$C(z) = (C_t - C_b)\left[1 - \cos\frac{\pi}{2}\left(\frac{2z+h}{2h}\right)\right] + C_b \tag{5b}$$

In addition, the temperature distribution obtained from Fourier equation of steady-state one-dimensional heat conduction is also considered:

$$T(z) = T_b + \frac{T_t - T_b}{\int_{-h/2}^{h/2}\frac{1}{k(z)}dz}\int_{-h/2}^{z}\frac{1}{k(\xi)}d\xi \tag{6}$$

2.3. Kinematics

The displacement field is chosen from previous study [25]:

$$u_1(x,z,t) = u(x,t) - zw_{,x} + \left[\sinh^{-1}\left(\frac{z}{h}\right) - \frac{8z^3}{3\sqrt{5}h^3}\right]\theta(x,t) = u(x,t) - zw_{,x} + f_1(z)\theta(x,t) \tag{7a}$$

$$u_3(x,z,t) = w(x,t) + \left(\frac{1}{\sqrt{h^2+z^2}} - \frac{8z^2}{\sqrt{5}h^3}\right)w_z(x,t) = w(x,t) + f_2(z)w_z(x,t) \tag{7b}$$

where the comma indicates partial differentiation with respect to the coordinate subscript that follows; $f_2 = f_{1,z}$; u and θ **are the axial displacement and rotation; and** w **and** w_z **are the transverse displacements, respectively**.

The nonzero strains are given by:

$$\epsilon_{xx}(x,z,t) = u_{,x} - zw_{,xx} + f_1\theta_{,x} \tag{8a}$$

$$\epsilon_{zz}(x,z,t) = f_{2,z}w_z \tag{8b}$$

$$\gamma_{xz}(x,z,t) = f_2\left(\theta + w_{z,x}\right) \tag{8c}$$

4

The elastic constitutive equations are given by:

$$
\left\{
\begin{array}{c}
\sigma_{xx} \\
\sigma_{zz} \\
\sigma_{xz}
\end{array}
\right\}
=
\left[
\begin{array}{ccc}
Q_{11} & Q_{13} & 0 \\
Q_{13} & Q_{11} & 0 \\
0 & 0 & Q_{55}
\end{array}
\right]
\left\{
\begin{array}{c}
\epsilon_{xx} \\
\epsilon_{zz} \\
\gamma_{xz}
\end{array}
\right\}
\tag{9}
$$

where

$$
Q_{11} = \frac{E(z)}{1-\nu^2}, \quad Q_{13} = \frac{E(z)\nu}{1-\nu^2}, \quad Q_{55} = \frac{E(z)}{2(1+\nu)}
\tag{10}
$$

If the transverse normal strain effect is omitted ($\epsilon_{zz} = 0$), the components of Q_{ij} in Eq. (9) are reduced as:

$$
Q_{11} = \frac{E(z)}{1-\nu^2}, \quad Q_{13} = 0, \quad Q_{55} = \frac{E(z)}{2(1+\nu)}
\tag{11}
$$

It is noted that Poisson's ratio ν is supposed to be constant through the beam thickness and its value is evaluated as the average of ceramic and metal ones.

2.4. Lagrange's equations

The strain energy $\mathcal{U}$ of system is expressed by:

$$
\begin{aligned}
\mathcal{U} &= \frac{1}{2} \int_V (\sigma_{xx}\epsilon_{xx} + \sigma_{zz}\epsilon_{zz} + \sigma_{xz}\gamma_{xz}) dV \\
&= \frac{1}{2} \int_0^L \Big[A u_{,x}^2 - 2B u_{,x} w_{,xx} + D w_{,xx}^2 + 2B^s u_{,x}\theta_{,x} - 2D^s w_{,xx}\theta_{,x} + H^s \theta_{,x}^2 \\
&\quad + 2(X u_{,x} w_z - Y w_{,xx} w_z + Y^s \theta_{,x} w_z) + Z w_z^2 + A^s(\theta^2 + 2\theta w_{z,x} + w_{z,x}^2) \Big] dx
\end{aligned}
\tag{12}
$$

where

$$
(A, B, D, B^s, D^s, H^s, Z) = \int_{-h/2}^{h/2} Q_{11}(z)\left(1, z, z^2, f_1, z f_1, f_1^2, f_{2,z}^2\right) b\, dz
\tag{13a}
$$

$$
(X, Y, Y^s) = \int_{-h/2}^{h/2} Q_{13}(z)\left(1, z, f_1\right) f_{2,z} b\, dz
\tag{13b}
$$

$$
A^s = \int_{-h/2}^{h/2} Q_{55}(z) f_2^2 b\, dz
\tag{13c}
$$

The work done $\mathcal{V}$ by axial hygro-thermal stress resultants is expressed by:

$$
\mathcal{V} = -\frac{1}{2} \int_0^L (N^t + N^m)(w_{,x})^2 dx
\tag{14}
$$

5

where

$$N^t = \int_{-h/2}^{h/2} Q_{11}(z)\alpha(z)\left[T(z) - T^0\right]bdz \tag{15a}$$

$$N^m = \int_{-h/2}^{h/2} Q_{11}(z)\beta(z)\left[C(z) - C^0\right]bdz \tag{15b}$$

The kinetic energy $\mathcal{K}$ is expressed by:

$$
\begin{aligned}
\mathcal{K} &= \frac{1}{2}\int_V \rho(z)(\dot{u}_1^2 + \dot{u}_3^2)dV \\
&= \frac{1}{2}\int_0^L \Big[I_0\dot{u}^2 - 2I_1\dot{u}\dot{w}_{,x} + I_2\dot{w}_{,x}^2 + 2J_1\dot{\theta}\dot{u} - 2J_2\dot{\theta}\dot{w}_{,x} + K_2\dot{\theta}^2 + I_0\dot{w}^2 \\
&\quad + 2L_1\dot{w}\dot{w}_z + L_2\dot{w}_z^2\Big]dx
\end{aligned} \tag{16}
$$

where dot-superscript denotes the differentiation with the time t; and $I_0, I_1, I_2, J_1, J_2, K_2, L_1, L_2$ are the inertia coefficients defined by:

$$(I_0, I_1, I_2, J_1, J_2, K_2, L_1, L_2) = \int_{-h/2}^{h/2} \rho(z)\left(1, z, z^2, f_1, zf_1, f_1^2, f_2, f_2^2\right)bdz \tag{17}$$

Lagrangian functional is used to derive the governing equations of motion:

$$\Pi = \mathcal{U} + \mathcal{V} - \mathcal{K} \tag{18}$$

$$
\begin{aligned}
\Pi &= \frac{1}{2}\int_0^L \Big[Au_{,x}^2 - 2Bu_{,x}w_{,xx} + Dw_{,xx}^2 + 2B^s u_{,x}\theta_{,x} - 2D^s w_{,xx}\theta_{,x} + H^s\theta_{,x}^2 \\
&\quad + 2(Xu_{,x}w_z - Yw_{,xx}w_z + Y^s\theta_{,x}w_z) + Zw_z^2 + A^s(\theta^2 + 2\theta w_{z,x} + w_{z,x}^2)\Big]dx \\
&\quad - \frac{1}{2}\int_0^L (N^t + N^m)(w_{,x})^2 dx \\
&\quad - \frac{1}{2}\int_0^L \Big[I_0\dot{u}^2 - 2I_1\dot{u}\dot{w}_{,x} + I_2\dot{w}_{,x}^2 + 2J_1\dot{\theta}\dot{u} - 2J_2\dot{\theta}\dot{w}_{,x} + K_2\dot{\theta}^2 + I_0\dot{w}^2 + 2L_1\dot{w}\dot{w}_z + L_2\dot{w}_z^2\Big]dx
\end{aligned} \tag{19}
$$

The displacement field is expressed by the approximation functions according to the Ritz method as follows:

$$u(x,t) = \sum_{j=1}^N u_j\psi_j(x)e^{i\omega t} \tag{20a}$$

$$w(x,t) = \sum_{j=1}^N w_j\varphi_j(x)e^{i\omega t} \tag{20b}$$

$$\theta(x,t) = \sum_{j=1}^N \theta_j\psi_j(x)e^{i\omega t} \tag{20c}$$

$$w_z(x,t) = \sum_{j=1}^N y_j\varphi_j(x)e^{i\omega t} \tag{20d}$$

6

where ω is the natural frequency, and $(u_j, w_j, \theta_j, y_j)$ are unknown values. The approximation functions $\psi_j(x)$ and $\varphi_j(x)$ are chosen as follows:

$$\psi_j(x) = \varphi_j(x) = x^{j-1} \tag{21}$$

The Lagrange multipliers (δ_i) are used to impose the boundary conditions, that leads to a new Lagrangian functional:

$$\Pi^* = \Pi + \delta_i \bar{u}_i(\bar{x}) \tag{22}$$

where $\bar{u}_i(\bar{x})$ denote prescribed displacement at two ends ($\bar{x} = 0$ and L). Substituting Eq. (20) into Eq. (19), and using Lagrange's equations:

$$\frac{\partial \Pi}{\partial q_j} - \frac{d}{dt} \frac{\partial \Pi}{\partial \dot{q}_j} = 0 \tag{23}$$

where q_j representing the values of $(u_j, w_j, \theta_j, y_j)$, a characteristic problem for hygro-thermal vibration and buckling response is obtained through the stiffness matrix $\mathbf{K}$ and mass matrix $\mathbf{M}$:

$$\left(\begin{bmatrix} \mathbf{K}^{11} & \mathbf{K}^{12} & \mathbf{K}^{13} & \mathbf{K}^{14} & \mathbf{K}^{15} \\ {}^T\mathbf{K}^{12} & \mathbf{K}^{22} & \mathbf{K}^{23} & \mathbf{K}^{24} & \mathbf{K}^{25} \\ {}^T\mathbf{K}^{13} & {}^T\mathbf{K}^{23} & \mathbf{K}^{33} & \mathbf{K}^{34} & \mathbf{K}^{35} \\ {}^T\mathbf{K}^{14} & {}^T\mathbf{K}^{24} & {}^T\mathbf{K}^{34} & \mathbf{K}^{44} & \mathbf{K}^{45} \\ {}^T\mathbf{K}^{15} & {}^T\mathbf{K}^{25} & {}^T\mathbf{K}^{35} & {}^T\mathbf{K}^{45} & \mathbf{0} \end{bmatrix} - \omega^2 \begin{bmatrix} \mathbf{M}^{11} & \mathbf{M}^{12} & \mathbf{M}^{13} & \mathbf{0} & \mathbf{0} \\ {}^T\mathbf{M}^{12} & \mathbf{M}^{22} & \mathbf{M}^{23} & \mathbf{M}^{24} & \mathbf{0} \\ {}^T\mathbf{M}^{13} & {}^T\mathbf{M}^{23} & \mathbf{M}^{33} & \mathbf{0} & \mathbf{0} \\ \mathbf{0} & {}^T\mathbf{M}^{24} & \mathbf{0} & \mathbf{M}^{44} & \mathbf{0} \\ \mathbf{0} & \mathbf{0} & \mathbf{0} & \mathbf{0} & \mathbf{0} \end{bmatrix} \right) \left\{ \begin{array}{c} \mathbf{u} \\ \mathbf{w} \\ \boldsymbol{\theta} \\ \mathbf{y} \\ \boldsymbol{\delta} \end{array} \right\} = \left\{ \begin{array}{c} \mathbf{0} \\ \mathbf{0} \\ \mathbf{0} \\ \mathbf{0} \\ \mathbf{0} \end{array} \right\} \tag{24}$$

where

$$K_{ij}^{11} = A \int_0^L \psi_{i,x} \psi_{j,x} \, dx, \, K_{ij}^{12} = -B \int_0^L \psi_{i,x} \varphi_{j,xx} \, dx, \, K_{ij}^{13} = B^s \int_0^L \psi_{i,x} \psi_{j,x} \, dx$$

$$K_{ij}^{14} = X \int_0^L \psi_{i,x} \varphi_j \, dx, \, K_{ij}^{22} = D \int_0^L \varphi_{i,xx} \varphi_{j,xx} \, dx - N^t \int_0^L \varphi_{i,x} \varphi_{j,x} \, dx - N^m \int_0^L \varphi_{i,x} \varphi_{j,x} \, dx$$

$$K_{ij}^{23} = -D^s \int_0^L \varphi_{i,xx} \psi_{j,x} \, dx, \, K_{ij}^{24} = -Y \int_0^L \varphi_{i,xx} \varphi_j \, dx$$

$$K_{ij}^{33} = H^s \int_0^L \psi_{i,x} \psi_{j,x} \, dx + A^s \int_0^L \psi_i \psi_j \, dx, \, K_{ij}^{34} = Y^s \int_0^L \psi_{i,x} \varphi_j \, dx + A^s \int_0^L \psi_i \varphi_{j,x} \, dx$$

$$K_{ij}^{44} = Z \int_0^L \varphi_i \varphi_j \, dx + A^s \int_0^L \varphi_{i,x} \varphi_{j,,x} \, dx$$

$$M_{ij}^{11} = I_0 \int_0^L \psi_i \psi_j \, dx, \, M_{ij}^{12} = -I_1 \int_0^L \psi_i \varphi_{j,x} \, dx, \, M_{ij}^{13} = J_1 \int_0^L \psi_i \psi_j \, dx$$

$$M_{ij}^{22} = I_0 \int_0^L \varphi_i \varphi_j \, dx + I_2 \int_0^L \varphi_{i,x} \varphi_{j,x} \, dx, \, M_{ij}^{23} = -J_2 \int_0^L \varphi_{i,x} \psi_j \, dx$$

$$M_{ij}^{24} = L_1 \int_0^L \varphi_i \varphi_j \, dx, \, M_{ij}^{33} = K_2 \int_0^L \psi_i \psi_j \, dx, \, M_{ij}^{44} = L_2 \int_0^L \psi_i \psi_j \, dx \tag{25}$$

The components of matrix $\mathbf{K}^{15}$, $\mathbf{K}^{25}$, $\mathbf{K}^{35}$ and $\mathbf{K}^{45}$, which depend on boundary conditions (Table 2), are list below:

- For hinged-hinged (H-H) beams:

$$
\begin{aligned}
K_{i1}^{15} &= \psi_i(0), \; K_{i2}^{15} = \psi_i(L), \; K_{ij}^{15} = 0 \quad \text{with } j = 3, 4, ..., 6 \\
K_{i3}^{25} &= \varphi_i(0), \; K_{i4}^{25} = \varphi_i(L), \; K_{ij}^{25} = 0 \quad \text{with } j = 1, 2, 5, 6 \\
K_{ij}^{35} &= 0 \quad \text{with } j = 1, 2, ..., 6 \\
K_{i5}^{45} &= \varphi_i(0), \; K_{i6}^{45} = \varphi_i(L), \; K_{ij}^{45} = 0 \quad \text{with } j = 1, 2, 3, 4
\end{aligned}
\tag{26}
$$

- For clamped-hinged (C-H) beams:

$$
\begin{aligned}
K_{i1}^{15} &= \psi_i(0), \; K_{i2}^{15} = \psi_i(L), \; K_{ij}^{15} = 0 \quad \text{with } j = 3, 4, ..., 8 \\
K_{i3}^{25} &= \varphi_i(0), \; K_{i4}^{25} = \varphi_i(L), \; K_{i5}^{25} = \varphi_{i,x}(0), \; K_{ij}^{25} = 0 \quad \text{with } j = 1, 2, 6, 7, 8 \\
K_{i6}^{35} &= \psi_i(0), \; K_{ij}^{35} = 0 \quad \text{with } j = 1, 2, 3, 4, 5, 7, 8 \\
K_{i7}^{45} &= \varphi_i(0), \; K_{i8}^{45} = \varphi_i(L), \; K_{ij}^{45} = 0 \quad \text{with } j = 1, 2, ..., 6
\end{aligned}
\tag{27}
$$

- For clamped-clamped (C-C) beams:

$$
\begin{aligned}
K_{i1}^{15} &= \psi_i(0), \; K_{i2}^{15} = \psi_i(L), \; K_{ij}^{15} = 0 \quad \text{with } j = 3, 4, ..., 10 \\
K_{i3}^{25} &= \varphi_i(0), \; K_{i4}^{25} = \varphi_i(L), \; K_{i5}^{25} = \varphi_{i,x}(0), \; K_{i6}^{25} = \varphi_{i,x}(L), \; K_{ij}^{25} = 0 \quad \text{with } j = 1, 2, 7, ..., 10 \\
K_{i7}^{35} &= \psi_i(0), \; K_{i8}^{35} = \psi_i(L), \; K_{ij}^{35} = 0 \quad \text{with } j = 1, 2, ..., 6, 9, 10 \\
K_{i9}^{45} &= \varphi_i(0), \; K_{i10}^{45} = \varphi_i(L), \; K_{ij}^{45} = 0 \quad \text{with } j = 1, 2, ..., 8
\end{aligned}
\tag{28}
$$

3. Numerical results and discussion

In this section, a number of numerical examples are analyzed to verify the accuracy of present theory and investigate the effects of power-law index, span-to-depth ratio, transverse normal strain, temperature and moisture content on buckling and vibration responses of FG beams for various boundary conditions (H-H, C-H and C-C). FG beams are made of ceramic (Si_3N_4, Al_2O_3) and metal (SUS304) with material properties in Table 1. Three types of temperature and moisture distribution through the beam depth are considered: uniform moisture and temperature rise (UMR, UTR), linear moisture and temperature rise (LMR, LTR), nonlinear moisture and temperature rise (NLMR, NLTR). The following non-dimensional parameters are used:

$$
\bar{\omega} = \frac{\omega L^2}{h} \sqrt{\frac{I_0}{\int_{-h/2}^{h/2} E(z) dz}}, \; \hat{\omega} = \frac{\omega L^2}{h} \sqrt{\frac{12\rho_c}{E_c}}, \; \lambda = \Delta T_{cr} \frac{L^2}{h^2} \alpha_m
\tag{29}
$$

where α_m is thermal expansion coefficient of metal at T_0 (K). Noticing that the following relations are used in this paper: T_0=300 (K), C_0=0 %, T_b - T_0=5 (K).

For convergence test, Table 3 reports the first natural frequency with respect to the number of series N of Si_3N_4/SUS304 beams with p=1, L/h=5 and ΔT=20, ΔC=0. The results are calculated with different boundary conditions and Fourier-law NLTR. In order to obtain good solution, the number of series N are chosen 8, 12, and 14 for H-H, C-H and C-C beams, respectively. For this reason, these numbers are used in the following examples.

As the first example, FG beams under uniform temperature rise (UTR) are considered. Table 4 presents the normalized critical temperatures of Si_3N_4/SUS304 beams for both temperature dependency (TD) and temperature independency (TID) solutions with different values of power-law index p. It is noted that the results reported in this example are based on the assumption that the temperature resultant in Eq. (15a) is calculated with $Q_{11} = E(z)/(1 - \nu)$. The results are compared with those of Wattanasakulpong et al. [33] and Trinh et al. [35] using HSBT. The present results without normal strain ($\epsilon_{zz} = 0$) are in good agreement with earlier works. Figure 2a presents the effect of the power-law index p on the normalized critical temperatures of Si_3N_4/SUS304 beams with L/h=20. It is plotted with both TD and TID solutions as well as with and without normal strain. It can be seen that the normalized critical temperatures decrease with the increase of p and the results with $\epsilon_{zz} \neq 0$ are smaller than those with $\epsilon_{zz} = 0$. This can be explained by the fact that the effect of transverse normal strain made beams softer. This figure also shows that the TD solutions give lower values than the TID ones, which emphasizes the importance of temperature dependency in the FG beams. Similarly, the accuracy of present theory in predicting the vibration response of Al_2O_3/SUS304 FG beams is studied in Table 5. The results are calculated with p=0.2, 2 and ΔT=0, 50 and 100. It is seen that good agreements between HSBTs are again found for all cases. Figure 2b displays the effects of UTR on the normalized fundamental frequency of Al_2O_3/SUS304 FG beams (L/h=30 and p=2). Obviously, the result decreases with the increase of ΔT up to critical temperatures at which the fundamental frequencies vanish. In this case, the critical temperatures of H-H, C-H and C-C beams are 52.6580 (K), 103.5923 (K) and 192.1833 (K), respectively.

The next example aims to investigate the effects of linear and nonlinear temperature rise (LTR, NLTR) on the thermal buckling and vibration of FG beams. For verification purpose, the critical temperatures of Si_3N_4/SUS304 beams with L/h=40 are reported in Table 6. These results are compared with those of Esfahani et al. [28], Ebrahimi and Salari [2] based on FSDT. It is observed that the present solutions are in good agreement with those of [28] for C-C beams under the Fourier-law NLTR while there is slight deviations for several values of p between the present solutions and those of [2]

9

for H-H beams under LTR. It is noted that the superscript "a" is used to indicate that Poisson's ratio effect is not included in the constitutive equation and thermal stress resultant ($Q_{11} = E(z)$) and this index will be used in the next examples for verification studies. Tables 7 and 8 show the comparisons of the critical temperatures from the present solutions and those from [35]. It shows that there are small differences between the HSBT models. The effect of normal strain is again found in which the HSBTs over-predict critical temperatures in comparison with the quasi-3D theory. Figure 3a displays the variation of fundamental frequency for UTR, LTR and Fourier-law NLTR. It can be seen that the results decrease with the increase of ΔT and vanish at the critical temperatures. Table 9 and Figure 3b consider the effects of temperature distribution under Fourier- and sinusoidal-law through the beam depth for different boundary conditions. For comparison, the critical temperature with Fourier law is smaller than that with sinusoidal one. Moreover, Table 10 presents the normalized fundamental frequency of Si_3N_4/SUS304 beams with L/h=20, p=0.1, 0.5 and 1, ΔT=20 and 80, subjected to the LTR and Fourier-law NLTR. The results are compared to those of [33] and [35] for different boundary conditions and good agreements between the HSBT models are again found.

The final example is to analyse the effects of moisture content on the thermal vibration behaviour of FG beams. Tables 11-13 present the normalized fundamental frequencies of Si_3N_4/SUS304 FG beams under the uniform, linear and nonlinear moisture (UMR, LMR, NLMR) and temperature rises. It is noted that the sinusoidal-law NLMR is used in this example. The results are calculated for the power-law indices p=0.2, 1 and 5, ΔT=0, 20 and 40, ΔC=0 %,1 % and 2 %. The present solutions are compared with those obtained from Ebrahimi and Barati [3] based on HSBT with H-H beam. The present solutions based on HSBT without Poisson's ratio are in good agreement with those of [3] for all moisture and temperature changes. The effect of normal strain is clearly observed in which the quasi-3D solutions are smaller the HSBT ones. Figure 4a presents the effect of the power-law index p on the normalized fundamental frequency of Si_3N_4/SUS304 FG beams (L/h=20) with different values of ΔC. It shows that for a moisture rise, the fundamental frequency decreases with the increase of p and the moisture content rise makes the beams softer. This phenomena is also observed in Fig. 4b which plots the variation of fundamental frequency with respect to the UTR. It can be seen from this figure that the frequency of the FG beams with moisture content rise ΔC=2% is smaller than that without moisture content rise, and that the critical temperatures decrease with the increase of ΔC.

4. Conclusions

Hygro-thermal vibration and stability analysis of FG beams is presented. It is based on a higher-order shear deformation theory, which considers a higher-order distribution of transverse shear stress

and both in-plane and out-of-plane displacements. These beams are subjected to hygro-thermal loadings under uniform, linear and nonlinear distributions through the beam depth. Lagrange's equations are applied to derive the characteristic dynamic equations and Ritz solution method is developed to solve the problems for different boundary conditions. The proposed Ritz solution converges quickly and agrees well with that from other studies. The obtained numerical results showed that:

- The critical buckling temperatures and natural frequencies derived from the quasi-3D theory, which includes normal strain, is smaller than those from the HSBT, which neglects it. It implies that the effect of normal strain is important and needs to be taken into account for the analysis of hygro-thermal behaviours of FG beams.

- The increase of the power-law index leads to the increase of metal volume fraction, that makes the beams softer and decrease of the critical temperature and natural frequency.

- The temperature dependency solutions give lower values than the temperature independency ones, so the importance of temperature dependency in the FG beams is confirmed.

- For a temperature rise, the critical temperature and fundamental frequency derived from nonlinear temperature rise are larger than those from uniform one.

- The critical temperature and fundamental frequency calculated from Fourier-law nonlinear temperature distribution are smaller than those from sinusoidal-law one.

- The thermal buckling and vibration responses of FG beams decrease with the increase of moisture content.

In conclusion, the proposed beam model and approach is found to be simply and efficient for hygro-thermal buckling and vibration of FG beams.

References

[1] F. Ebrahimi, E. Salari, Nonlocal thermo-mechanical vibration analysis of functionally graded nanobeams in thermal environment, Acta Astronautica 113 (2015) 29 – 50.

[2] F. Ebrahimi, E. Salari, Thermal buckling and free vibration analysis of size dependent Timoshenko FG nanobeams in thermal environments, Composite Structures 128 (2015) 363 – 380.

[3] F. Ebrahimi, M. R. Barati, A unified formulation for dynamic analysis of nonlocal heterogeneous nanobeams in hygro-thermal environment, Applied Physics A 122 (9) (2016) 792.

[4] M. Zidi, A. Tounsi, M. S. A. Houari, E. A. A. Bedia, O. A. Beg, Bending analysis of FGM plates under hygro-thermo-mechanical loading using a four variable refined plate theory, Aerospace Science and Technology 34 (2014) 24 – 34.

[5] A. M. Zenkour, Hygro-thermo-mechanical effects on FGM plates resting on elastic foundations, Composite Structures 93 (1) (2010) 234 – 238.

[6] A. M. Zenkour, M. N. M. Allam, A. F. Radwan, Effects of transverse shear and normal strains on FG plates resting on elastic foundations under hygro-thermo-mechanical loading, International Journal of Applied Mechanics 06 (05) (2014) 1450063.

[7] F. A. Fazzolari, E. Carrera, Thermal stability of FGM sandwich plates under various through-the-thickness temperature distributions, Journal of Thermal Stresses 37 (12) (2014) 1449–1481.

[8] M. Aydogdu, V. Taskin, Free vibration analysis of functionally graded beams with simply supported edges, Materials and Design 28 (2007) 1651–1656.

[9] K. Pradhan, S. Chakraverty, Free vibration of Euler and Timoshenko functionally graded beams by Rayleigh-Ritz method, Composites Part B: Engineering 51 (2013) 175 – 184.

[10] A. Chakraborty, S. Gopalakrishnan, J. N. Reddy, A new beam finite element for the analysis of functionally graded materials, International Journal of Mechanical Sciences 45 (3) (2003) 519 – 539.

[11] X.-F. Li, A unified approach for analyzing static and dynamic behaviors of functionally graded Timoshenko and Euler-Bernoulli beams, Journal of Sound and Vibration 318 (45) (2008) 1210 – 1229.

[12] S. Sina, H. Navazi, H. Haddadpour, An analytical method for free vibration analysis of functionally graded beams, Materials and Design 30 (3) (2009) 741 – 747.

[13] S.-R. Li, R. C. Batra, Relations between buckling loads of functionally graded Timoshenko and homogeneous Euler-Bernoulli beams, Composite Structures 95 (2013) 5 – 9.

[14] T.-K. Nguyen, T. P. Vo, H.-T. Thai, Static and free vibration of axially loaded functionally graded beams based on the first-order shear deformation theory, Composites Part B: Engineering 55 (2013) 147 – 157.

[15] S. Kapuria, M. Bhattacharyya, A. N. Kumar, Bending and free vibration response of layered functionally graded beams: A theoretical model and its experimental validation, Composite Structures 82 (3) (2008) 390 – 402.

[16] X.-F. Li, B.-L. Wang, J.-C. Han, A higher-order theory for static and dynamic analyses of functionally graded beams, Archive of Applied Mechanics 80 (2010) 1197–1212.

[17] T. P. Vo, H.-T. Thai, T.-K. Nguyen, F. Inam, Static and vibration analysis of functionally graded beams using refined shear deformation theory, Meccanica 49 (1) (2014) 155–168.

[18] T. P. Vo, H.-T. Thai, T.-K. Nguyen, A. Maheri, J. Lee, Finite element model for vibration and buckling of functionally graded sandwich beams based on a refined shear deformation theory, Engineering Structures 64 (2014) 12 – 22.

[19] H. T. Thai, T. P. Vo, Bending and free vibration of functionally graded beams using various higher-order shear deformation beam theories, International Journal of Mechanical Sciences 62 (1) (2012) 57–66.

[20] M. Simsek, Fundamental frequency analysis of functionally graded beams by using different higher-order beam theories, Nuclear Engineering and Design 240 (4) (2010) 697 – 705.

[21] G. Giunta, S. Belouettar, E. Carrera, Analysis of FGM Beams by Means of Classical and Advanced Theories, Mechanics of Advanced Materials and Structures 17 (8) (2010) 622–635.

[22] D. S. Mashat, E. Carrera, A. M. Zenkour, S. A. A. Khateeb, M. Filippi, Free vibration of FGM layered beams by various theories and finite elements, Composites Part B: Engineering 59 (2014) 269 – 278.

[23] A. I. Osofero, T. P. Vo, T.-K. Nguyen, J. Lee, Analytical solution for vibration and buckling of functionally graded sandwich beams using various quasi-3d theories, Journal of Sandwich Structures & Materials 18 (1) (2016) 3–29.

[24] T.-K. Nguyen, T. T.-P. Nguyen, T. P. Vo, H.-T. Thai, Vibration and buckling analysis of functionally graded sandwich beams by a new higher-order shear deformation theory, Composites Part B: Engineering 76 (2015) 273 – 285.

[25] T.-K. Nguyen, B.-D. Nguyen, A new higher-order shear deformation theory for static, buckling and free vibration analysis of functionally graded sandwich beams, Journal of Sandwich Structures & Materials 17 (6) (2015) 613–631.

[26] T.-K. Nguyen, T. P. Vo, B.-D. Nguyen, J. Lee, An analytical solution for buckling and vibration analysis of functionally graded sandwich beams using a quasi-3d shear deformation theory, Composite Structures 156 (2016) 238 – 252, 70th Anniversary of Professor J. N. Reddy.

[27] J. Yarasca, J. Mantari, R. Arciniega, Hermitelagrangian finite element formulation to study functionally graded sandwich beams, Composite Structures 140 (2016) 567 – 581.

[28] S. Esfahani, Y. Kiani, M. Eslami, Non-linear thermal stability analysis of temperature dependent FGM beams supported on non-linear hardening elastic foundations, International Journal of Mechanical Sciences 69 (2013) 10 – 20.

[29] S. Ghiasian, Y. Kiani, M. Eslami, Nonlinear thermal dynamic buckling of FGM beams, European Journal of Mechanics - A/Solids 54 (2015) 232 – 242.

[30] L. S. Ma, D. W. Lee, Exact solutions for nonlinear static responses of a shear deformable FGM beam under an in-plane thermal loading, European Journal of Mechanics A/Solids 31 (2012) 13–20.

[31] P. Malekzadeh, S. M. Monajjemzadeh, Dynamic response of functionally graded beams in a thermal environment under a moving load, Mechanics of Advanced Materials and Structures 23 (3) (2016) 248–258.

[32] B. V. Sankar, Thermal stresses in functionally graded beams, AIAA Journal 40 (6) (2002) 1228 – 1232.

[33] N. Wattanasakulpong, B. G. Prusty, D. W. Kelly, Thermal buckling and elastic vibration of third-order shear deformable functionally graded beams, International Journal of Mechanical Sciences 53 (2011) 734–743.

[34] Y. Sun, S.-R. Li, R. C. Batra, Thermal buckling and post-buckling of fgm timoshenko beams on nonlinear elastic foundation, Journal of Thermal Stresses 39 (1) (2016) 11–26.

[35] L. C. Trinh, T. P. Vo, H.-T. Thai, T.-K. Nguyen, An analytical method for the vibration and buckling of functionally graded beams under mechanical and thermal loads, Composites Part B: Engineering 100 (2016) 152 – 163.

[36] R. K. Bhangale, N. Ganesan, Thermoelastic buckling and vibration behaior of functionally graded sandwich beam with constrained viscoelastic core, Journal of Sound and Vibration 295 (2006) 294–316.

[37] S. Pradhan, T. Murmu, Thermo-mechanical vibration of FGM sandwich beam under variable elastic foundations using differential quadrature method, Journal of Sound and Vibration 321 (1-2) (2009) 342 – 362.

[38] H.-S. Shen, Nonlinear analysis of functionally graded fiber reinforced composite laminated beams in hygrothermal environments, part i: Theory and solutions, Composite Structures 125 (2015) 698 – 705.

[39] H.-S. Shen, Nonlinear analysis of functionally graded fiber reinforced composite laminated beams in hygrothermal environments, part ii: Numerical results, Composite Structures 125 (2015) 706 – 712.

[40] M. Aydogdu, Vibration analysis of cross-ply laminated beams with general boundary conditions by Ritz method, International Journal of Mechanical Sciences 47 (11) (2005) 1740 – 1755.

[41] M. Aydogdu, Buckling analysis of cross-ply laminated beams with general boundary conditions by Ritz method, Composites Science and Technology 66 (10) (2006) 1248 – 1255.

[42] M. Aydogdu, Free vibration analysis of angle-ply laminated beams with general boundary conditions, Journal of Reinforced Plastics and Composites 25 (15) (2006) 1571–1583.

[43] J. Mantari, F. Canales, Free vibration and buckling of laminated beams via hybrid Ritz solution for various penalized boundary conditions, Composite Structures 152 (2016) 306 – 315.

[44] T.-K. Nguyen, N.-D. Nguyen, T. P. Vo, H.-T. Thai, Trigonometric-series solution for analysis of laminated composite beams, Composite Structures 160 (2017) 142 – 151.

CAPTIONS OF TABLES

Table 1: Temperature dependent coefficients for ceramic and metal materials.

Table 2: Kinematic boundary conditions.

Table 3: Convergence test for the nondimensional fundamental frequency ($\hat{\omega}$) of Si_3N_4/SUS304 beams under Fourier-law NLTR with $p = 1$, $L/h = 20$, ΔT=20 (K), TD, ΔC=0 %.

Table 4: Normalized critical temperatures (λ) of Si_3N_4/SUS304 beams under UTR (L/h=20).

Table 5: Fundamental frequency ($\bar{\omega}$) of Al_2O_3/SUS304 beams under UTR (L/h=30).

Table 6: Critical temperature of Si_3N_4/SUS304 FG beams under LTR and Fourier-law NLTR (L/h=40, TD).

Table 7: Critical temperature of Si_3N_4/SUS304 FG beams under LTR for different boundary conditions (L/h=20, TD).

Table 8: Critical temperatures of Si_3N_4/SUS304 beams under Fourier-law NLTR (L/h=20, TD).

Table 9: Critical temperatures of Si_3N_4/SUS304 beams under Fourier- and sinusoidal-law NLTR (L/h=30, TD).

Table 10: Fundamental frequency ($\hat{\omega}$) of Si_3N_4/SUS304 beams under LTR and Fourier-law NLTR (L/h=20, TD).

Table 11: Fundamental frequency ($\hat{\omega}$) of Si_3N_4/SUS304 beams under uniform moisture and temperature rise for different boundary conditions (L/h=20, TD).

Table 12: Fundamental frequency ($\hat{\omega}$) of Si_3N_4/SUS304 beams under linear moisture and temperature rise (L/h=20, TD).

Table 13: Fundamental frequency ($\hat{\omega}$) of Si_3N_4/SUS304 beams under sinusoidal moisture and temperature rise(L/h=20, TD).

CAPTIONS OF FIGURES

Figure 1: Geometry of FG beams.

Figure 2: Variation of normalized critical temperature and fundamental frequency of FG beams with respect to the power-law index p and uniform temperature rise ΔT.

Figure 3: Variation of normalized fundamental frequency of Si_3N_4/SUS304 beams with respect to the power-law index p and temperature rise (TD).

Figure 4: Variation of normalized fundamental frequency of Si_3N_4/SUS304 beams with respect to the power-law index, moisture and temperature rise (L/h=20, TD).

Table 1: Temperature dependent coefficients for ceramic and metal materials.

Materials	P_0	P_{-1}	P_1	P_2	P_3
Al$_2$O$_3$					
E (Pa)	349.55e+9	0	-3.853e-4	4.027e-7	1.673e-10
α (1/K)	6.8269e-6	0	1.838e-4	0	0
β	0	0	0	0	0
κ (W/mK)	0.26	0	0	0	0
ν	0.26	0	0	0	0
ρ (kg/m^3)	3800	0	0	0	0
Si$_3$N$_4$					
E (Pa)	348.43e+9	0	-3.070e-4	2.160e-7	-8.946e-11
α (1/K)	5.8723e-6	0	9.095e-4	0	0
β	0	0	0	0	0
κ (W/mK)	13.723	0	-1.032e-3	5.466e-7	-7.876e-11
ν	0.24	0	0	0	0
ρ (kg/m^3)	2370	0	0	0	0
SUS304					
E (Pa)	201.04e+9	0	3.079e-4	-6.534e-7	0
α (1/K)	12.330e-6	0	8.086e-4	0	0
β	0.0005	0	0	0	0
κ (W/mK)	15.379	0	-1.264e-3	2.092e-6	-7.223e-10
ν	0.3262	0	-2.002e-4	3.797e-7	0
ρ (kg/m^3)	8166	0	0	0	0

Table 2: Kinematic boundary conditions.

BCs	$x = 0$	$x = L$
H-H	$u = 0$, $w = 0$, $w_z = 0$	$u = 0$, $w = 0$, $w_z = 0$
C-H	$u = 0$, $w = 0$, $w_{,x}=0$, $\theta=0$, $w_z = 0$	$u = 0$, $w = 0$, $w_z=0$,
C-C	$u = 0$, $w = 0$, $w_{,x}=0$, $\theta=0$, $w_z=0$	$u = 0$, $w = 0$, $w_{,x}=0$, $\theta=0$, $w_z=0$

Table 3: Convergence test for the nondimensional fundamental frequency ($\hat{\omega}$) of Si$_3$N$_4$/SUS304 beams under Fourier-law NLTR with $p = 1$, $L/h = 20$, ΔT=20 (K), TD, ΔC=0 %.

BCs	Normal strain	N						
		6	8	10	12	14	16	18
H-H	$\epsilon_{zz} = 0$	5.9735	5.9719	5.9719	5.9719	5.9719	5.9719	5.9719
	$\epsilon_{zz} \neq 0$	5.7193	5.7178	5.7178	5.7178	5.7178	5.7178	5.7178
C-H	$\epsilon_{zz} = 0$	9.4357	9.4283	9.4271	9.4265	9.4261	9.4259	9.4257
	$\epsilon_{zz} \neq 0$	9.1075	9.0795	9.0716	9.0678	9.0656	9.0640	9.0627
C-C	$\epsilon_{zz} = 0$	13.7367	13.7045	13.6990	13.6967	13.6953	13.6944	13.6938
	$\epsilon_{zz} \neq 0$	13.3787	13.2585	13.2321	13.2204	13.2140	13.2095	13.2057

Table 4: Normalized critical temperatures (λ) of Si$_3$N$_4$/SUS304 beams under UTR (L/h=20).

Temperature dependency	BCs	Theory	p					
			0	0.5	1	2	5	10
TID	H-H	Present ($\epsilon_{zz} = 0$)	1.309	0.970	0.878	0.812	0.752	0.714
		Present ($\epsilon_{zz} \neq 0$)	1.210	0.897	0.811	0.751	0.695	0.660
		HSBT [35]	1.307	-	0.866	-	0.744	0.710
		HSBT [33]	1.348	-	0.876	-	0.750	0.712
	C-C	Present ($\epsilon_{zz} = 0$)	5.133	3.780	3.399	3.136	2.918	2.784
		Present ($\epsilon_{zz} \neq 0$)	4.781	3.522	3.169	2.925	2.720	2.594
		HSBT [35]	5.130	-	3.398	-	2.917	2.782
	C-H	Present	2.656	1.958	1.763	1.628	1.514	1.443
		Present ($\epsilon_{zz} \neq 0$)	2.464	1.817	1.637	1.512	1.405	1.339
		HSBT [35]	2.654	-	1.758	-	1.510	1.440
TD	H-H	Present ($\epsilon_{zz} = 0$)	1.151	0.882	0.806	0.750	0.698	0.665
		Present ($\epsilon_{zz} \neq 0$)	1.071	0.820	0.748	0.696	0.648	0.617
		HSBT [35]	1.151	-	0.796	-	0.693	0.663
		HSBT [33]	1.185	-	0.805	-	0.697	0.664
	C-C	Present ($\epsilon_{zz} = 0$)	3.553	2.831	2.606	2.458	2.332	2.248
		Present ($\epsilon_{zz} \neq 0$)	3.336	2.663	2.456	2.313	2.190	2.102
		HSBT [35]	3.559	-	2.609	-	2.333	2.244
	C-H	Present ($\epsilon_{zz} = 0$)	2.116	1.644	1.506	1.408	1.324	1.269
		Present ($\epsilon_{zz} \neq 0$)	1.981	1.538	1.408	1.316	1.235	1.184
		HSBT [35]	2.115	-	1.503	-	1.321	1.267

Table 5: Fundamental frequency ($\bar{\omega}$) of Al$_2$O$_3$/SUS304 beams under UTR (L/h=30).

Temperature dependency	BCs	Theory	p=0.2			p=2		
			ΔT=0	50	100	ΔT=0	50	100
TID	H-H	Present ($\epsilon_{zz}=0$)	2.9484	1.8416	-	3.0100	1.1810	-
		Present ($\epsilon_{zz}\neq 0$)	2.8232	1.6347	-	2.8826	0.8051	-
		HSBT [35]	2.9506	1.8450	-	3.0129	1.1816	-
	C-C	Present ($\epsilon_{zz}=0$)	6.6373	6.1198	5.5490	6.7339	5.9821	5.1090
		Present ($\epsilon_{zz}\neq 0$)	6.3768	5.8352	5.2320	6.4732	5.6854	4.7553
		HSBT [35]	6.6371	6.1209	5.5489	6.7366	5.9834	5.1125
		HSBT [33]	6.6394	6.1189	5.5452	6.7355	5.9802	5.1028
	C-H	Present ($\epsilon_{zz}=0$)	4.5901	3.8552	2.9281	4.6625	3.5699	1.8886
		Present ($\epsilon_{zz}\neq 0$)	4.4056	3.6320	2.6236	4.4772	3.3216	1.3476
		HSBT [35]	4.5898	3.8574	2.9297	4.6653	3.5731	1.8925
TD	H-H	Present ($\epsilon_{zz}=0$)	2.9484	1.8191	-	3.0100	1.0859	-
		Present ($\epsilon_{zz}\neq 0$)	2.8232	1.6086	-	2.8826	0.6563	-
		HSBT [35]	2.9506	1.8220	-	3.0129	1.0868	-
	C-C	Present ($\epsilon_{zz}=0$)	6.6373	6.1124	5.5126	6.7339	5.9605	5.0032
		Present ($\epsilon_{zz}\neq 0$)	6.3768	5.8266	5.1905	6.4732	5.6616	4.6378
		HSBT [35]	6.6371	6.1142	5.5141	6.7366	5.9631	5.0068
		HSBT [33]	6.6394	6.1109	5.5081	6.7335	5.9581	4.9965
	C-H	Present ($\epsilon_{zz}=0$)	4.5901	3.8431	2.8594	4.6625	3.5347	1.5906
		Present ($\epsilon_{zz}\neq 0$)	4.4056	3.6185	2.5435	4.4772	3.2828	0.8707
		HSBT [35]	4.5898	3.8437	2.8608	4.6653	3.5391	1.5946

Table 6: Critical temperature of Si_3N_4/SUS304 FG beams under LTR and Fourier-law NLTR (L/h=40, TD).

Temperature distribution	BCs	Theory	p					
			0	0.5	1	2	5	10
LTR	H-H	Present[a] ($\epsilon_{zz} = 0$)	116.4406	91.8046	82.9295	75.8794	69.0474	64.8133
		FSBT [2]	127.3340	95.5739	84.6229	76.4715	69.4307	-
Fourier-law NLTR	C-C	Present[a] ($\epsilon_{zz} = 0$)	411.7059	377.7547	357.9741	337.0286	310.0925	291.3543
		FSBT [28]	412.2400	377.9600	357.9400	337.0300	310.1200	291.3500

[a]: $Q_{11} = E(z)$

Table 7: Critical temperature of Si_3N_4/SUS304 FG beams under LTR for different boundary conditions (L/h=20, TD).

BCs	Theory	p					
		0	0.5	1	2	5	10
H-H	Present ($\epsilon_{zz} = 0$)	411.5245	354.7101	332.6536	314.4494	295.2286	282.2571
	Present ($\epsilon_{zz} \neq 0$)	385.1274	330.2483	308.9443	291.3484	272.8943	260.5459
	Present[a] ($\epsilon_{zz} = 0$)	411.7060	354.8756	332.8174	314.6159	295.3957	282.4179
	HSBT [35]	451.5600	360.9400	328.1300	301.5600	279.6900	265.6300
C-C	Present ($\epsilon_{zz} = 0$)	1156.1584	1106.1719	1089.8592	1078.7302	1073.7643	1065.7153
	Present ($\epsilon_{zz} \neq 0$)	1100.9855	1046.4138	1027.9710	1014.8334	1006.9889	997.0252
	Present[a] ($\epsilon_{zz} = 0$)	1157.7996	1107.9445	1091.7181	1080.6962	1075.8608	1067.8635
	HSBT [35]	-	1142.1900	1062.5000	1004.6900	957.8100	921.8800
C-H	Present ($\epsilon_{zz} = 0$)	718.5718	652.8875	624.7796	604.3525	584.2301	568.0967
	Present ($\epsilon_{zz} \neq 0$)	679.1061	613.3336	585.5554	564.7903	544.1176	528.0379
	Present[a] ($\epsilon_{zz} = 0$)	719.2049	653.5143	625.4122	605.0142	584.9244	568.7844
	HSBT [35]	814.0600	667.1900	612.5000	570.3100	531.2500	507.8100

[a]: $Q_{11} = E(z)$

Table 8: Critical temperatures of Si$_3$N$_4$/SUS304 beams under Fourier-law NLTR (L/h=20, TD).

BCs	Theory	p					
		0	0.5	1	2	5	10
H-H	Present ($\epsilon_{zz} = 0$)	411.5245	379.3918	360.9977	340.3445	311.8557	291.9825
	Present ($\epsilon_{zz} \neq 0$)	385.1274	352.4187	334.2954	314.4406	287.6173	269.1585
	Present^a ($\epsilon_{zz} = 0$)	411.7060	379.5747	361.1826	340.5314	312.0370	292.1517
	HSBT [35]	451.5600	388.7500	357.5000	327.5000	293.7500	273.7500
C-C	Present ($\epsilon_{zz} = 0$)	1156.1584	1204.0415	1213.1728	1202.5179	1164.6606	1124.4957
	Present ($\epsilon_{zz} \neq 0$)	1100.9855	1140.8570	1146.0126	1133.6258	1093.7100	1052.6690
	Present^a ($\epsilon_{zz} = 0$)	1157.7996	1205.9121	1215.1809	1204.6140	1166.8631	1126.7276
	HSBT [35]	-	-	-	1132.5000	1042.5000	972.5000
C-H	Present ($\epsilon_{zz} = 0$)	718.5718	709.6778	695.0922	672.6986	630.3660	596.2206
	Present ($\epsilon_{zz} \neq 0$)	679.1061	666.0060	650.0307	627.0078	585.8770	553.3163
	Present^a ($\epsilon_{zz} = 0$)	719.2049	710.3689	695.8183	673.4623	631.1354	596.9569
	HSBT [35]	814.0600	736.2500	688.7500	637.5000	572.5000	531.2500

^{a}: $Q_{11} = E(z)$

Table 9: Critical temperatures of Si$_3$N$_4$/SUS304 beams under Fourier- and sinusoidal-law NLTR (L/h=30, TD).

Temperature distribution	BCs	Theory	p					
			0	0.5	1	2	5	10
Fourier	H-H	Present ($\epsilon_{zz} = 0$)	202.2578	173.5389	160.5549	148.3615	134.2035	125.0658
		Present ($\epsilon_{zz} \neq 0$)	187.7199	160.0195	147.7213	136.2821	123.1300	114.6789
	C-C	Present ($\epsilon_{zz} = 0$)	647.7525	630.7537	613.2717	589.7918	550.4308	519.7221
		Present ($\epsilon_{zz} \neq 0$)	611.2257	590.8552	572.5358	548.9211	510.9149	481.7654
	C-H	Present ($\epsilon_{zz} = 0$)	379.9401	345.7176	326.5833	306.6677	281.4281	264.1042
		Present ($\epsilon_{zz} \neq 0$)	355.7747	321.7415	302.8348	283.7695	259.9836	243.8099
Sinusoidal	H-H	Present ($\epsilon_{zz} = 0$)	266.8324	224.9764	208.1080	193.4138	178.0297	168.1896
		Present ($\epsilon_{zz} \neq 0$)	248.2054	208.2022	192.1421	178.2136	163.6644	154.4077
	C-C	Present ($\epsilon_{zz} = 0$)	823.1910	755.8429	727.9468	706.6631	687.8553	672.7974
		Present ($\epsilon_{zz} \neq 0$)	778.0221	710.9078	683.0384	661.3097	641.8079	625.5963
	C-H	Present ($\epsilon_{zz} = 0$)	491.8173	430.8636	406.2229	385.4767	364.4358	349.8751
		Present ($\epsilon_{zz} \neq 0$)	461.5226	402.6337	378.6681	358.7276	337.7749	323.6678

Table 10: Fundamental frequency ($\hat{\omega}$) of Si$_3$N$_4$/SUS304 beams under LTR and Fourier-law NLTR (L/h=20, TD).

Temperature distribution	BCs	Theory	ΔT(K)=20			ΔT(K)=80		
			p=0.1	0.5	1	p=0.1	0.5	1
LTR	H-H	Present ($\epsilon_{zz}=0$)	8.7846	6.8133	5.9658	8.1742	6.2547	5.4252
		Present ($\epsilon_{zz}\neq0$)	8.4170	6.5248	5.7113	7.7782	5.9387	5.1433
		Present^a ($\epsilon_{zz}=0$)	8.4391	6.5450	5.7307	7.8532	6.0088	5.2118
		HSBT [1]	8.4716	6.5742	5.7588	7.8766	6.0166	5.2128
		HSBT [35]	8.4634	6.5415	5.7114	7.8795	6.0063	5.1927
	C-C	Present ($\epsilon_{zz}=0$)	20.1188	15.6333	13.6920	19.8063	15.3661	13.4427
		Present ($\epsilon_{zz}\neq0$)	19.4059	15.0816	13.2106	19.0807	14.8018	12.9487
		Present^a ($\epsilon_{zz}=0$)	19.3522	15.0342	13.1654	19.0523	14.7779	12.9263
		HSBT [1]	19.6398	15.2580	13.3671	19.3420	15.0040	13.1304
		HSBT [35]	19.3371	15.0222	13.1554	18.9778	14.6972	12.8431
	C-H	Present ($\epsilon_{zz}=0$)	13.8663	10.7631	9.4225	13.4286	10.3728	9.0500
		Present ($\epsilon_{zz}\neq0$)	13.3426	10.3565	9.0669	12.8863	9.9482	8.6764
		Present^a ($\epsilon_{zz}=0$)	13.3283	10.3443	9.0552	12.9083	9.9697	8.6976
		HSBT [1]	13.4380	10.4238	9.1227	13.0201	10.0515	8.7674
		HSBT [35]	13.3373	10.3526	9.0635	12.8837	9.9342	8.6571
NLTR	H-H	Present ($\epsilon_{zz}=0$)	8.7865	6.8184	5.9719	8.1855	6.2841	5.4605
		Present ($\epsilon_{zz}\neq0$)	8.4190	6.5302	5.7178	7.7900	5.9696	5.1805
		Present^a ($\epsilon_{zz}=0$)	8.4409	6.5499	5.7366	7.8640	6.0370	5.2456
		HSBT [1]	8.4675	6.5437	5.7124	7.9265	6.0402	5.2186
		HSBT [35]	8.4730	6.5779	5.7632	7.8861	6.0431	5.2448
	C-C	Present ($\epsilon_{zz}=0$)	20.1198	15.6360	13.6953	19.8121	15.3810	13.4604
		Present ($\epsilon_{zz}\neq0$)	19.4070	15.0844	13.2140	19.0867	14.8172	12.9670
		Present^a ($\epsilon_{zz}=0$)	19.3532	15.0369	13.1685	19.0578	14.7921	12.9432
		HSBT [1]	19.6390	15.2501	13.3558	19.3552	14.9886	13.1011
		HSBT [35]	19.3379	15.0244	13.1579	18.9832	14.7115	12.8600
	C-H	Present ($\epsilon_{zz}=0$)	13.8676	10.7669	9.4271	13.4367	10.3935	9.0747
		Present ($\epsilon_{zz}\neq0$)	13.3441	10.3605	9.0716	12.8947	9.9698	8.7022
		Present^a ($\epsilon_{zz}=0$)	13.3297	10.3479	9.0595	12.9160	9.9896	8.7214
		HSBT [1]	13.4395	10.4211	9.1178	13.0483	10.0594	8.7648
		HSBT [35]	13.3382	10.3553	9.0669	12.8907	9.9533	8.6801

^{a}: $Q_{11} = E(z)$

Table 11: Fundamental frequency ($\hat{\omega}$) of Si$_3$N$_4$/SUS304 beams under uniform moisture and temperature rise for different boundary conditions (L/h=20, TD).

BCs	ΔC	Theory	ΔT=0			ΔT=20			ΔT=40		
			p=0.2	1	5	p=0.2	1	5	p=0.2	1	5
H-H	ΔC=0%	Present ($\epsilon_{zz}=0$)	8.3030	6.2144	5.0652	7.9313	5.8635	4.7304	7.5298	5.4784	4.3579
		Present ($\epsilon_{zz}\neq 0$)	7.9769	5.9708	4.8664	7.5893	5.6046	4.5168	7.1685	5.2003	4.1250
		Present[a] ($\epsilon_{zz}=0$)	7.9757	5.9694	4.8656	7.6186	5.6324	4.5441	7.2327	5.2624	4.1863
		HSBT [3]	7.9680	5.9314	4.8449	-	-	-	-	-	-
	ΔC=1%	Present ($\epsilon_{zz}=0$)	8.1372	5.8496	4.5711	7.7574	5.4749	4.1958	7.3463	5.0598	3.7699
		Present ($\epsilon_{zz}\neq 0$)	7.8043	5.5906	4.3504	7.4076	5.1971	3.9542	6.9757	4.7578	3.4988
		Present[a] ($\epsilon_{zz}=0$)	7.8164	5.6192	4.3913	7.4516	5.2593	4.0309	7.0566	4.8606	3.6219
		HSBT [3]	-	-	-	7.4435	5.2167	4.0063	-	-	-
	ΔC=2%	Present ($\epsilon_{zz}=0$)	7.9679	5.4606	4.0166	7.5796	5.0564	3.5824	7.1581	4.6033	3.0712
		Present ($\epsilon_{zz}\neq 0$)	7.6278	5.1826	3.7644	7.2213	4.7549	3.2969	6.7775	4.2697	2.7327
		Present[a] ($\epsilon_{zz}=0$)	7.6539	5.2457	3.8590	7.2809	4.8576	3.4421	6.8759	4.4224	2.9514
		HSBT [3]	-	-	-	-	-	-	6.8673	4.3722	2.9180
C-H	ΔC=0%	Present ($\epsilon_{zz}\neq 0$)	12.4092	9.2498	7.5477	12.1243	8.9822	7.2940	11.8230	8.6962	7.0206
	ΔC=1%	Present ($\epsilon_{zz}\neq 0$)	12.2809	8.9691	7.1716	11.9926	8.6917	6.9021	11.6876	8.3948	6.6106
	ΔC=2%	Present ($\epsilon_{zz}\neq 0$)	12.1512	8.6786	6.7731	11.8594	8.3905	6.4848	11.5505	8.0814	6.1715
C-C	ΔC=0%	Present ($\epsilon_{zz}\neq 0$)	17.9130	13.3399	10.8821	17.7061	13.1479	10.7012	17.4896	12.9450	10.5089
	ΔC=1%	Present ($\epsilon_{zz}\neq 0$)	17.8188	13.1346	10.6086	17.6106	12.9390	10.4218	17.3928	12.7321	10.2231
	ΔC=2%	Present ($\epsilon_{zz}\neq 0$)	17.7240	12.9258	10.3270	17.5146	12.7262	10.1338	17.2954	12.5153	9.9282

[a]: $Q_{11}=E(z)$

Table 12: Fundamental frequency ($\hat{\omega}$) of Si$_3$N$_4$/SUS304 beams under linear moisture and temperature rise (L/h=20, TD).

| BCs	ΔC	Theory	ΔT=0			ΔT=20			ΔT=40		
			p=0.2	1	5	p=0.2	1	5	p=0.2	1	5
H-H	ΔC=0%	Present ($\epsilon_{zz}=0$)	8.2127	6.1295	4.9846	8.0343	5.9658	4.8259	7.8474	5.7943	4.6597
		Present ($\epsilon_{zz}\neq0$)	7.8828	5.8824	4.7825	7.6969	5.7113	4.6164	7.5016	5.5317	4.4420
		Present^a ($\epsilon_{zz}=0$)	7.8889	5.8879	4.7882	7.7177	5.7307	4.6358	7.5382	5.5661	4.4763
		HSBT [3]	7.8817	5.8491	4.7664	-	-	-	-	-	-
	ΔC=1%	Present ($\epsilon_{zz}=0$)	8.1651	5.9992	4.7669	7.9857	5.8315	4.5999	7.7976	5.6558	4.4245
		Present ($\epsilon_{zz}\neq0$)	7.8334	5.7466	4.5554	7.6461	5.5711	4.3800	7.4495	5.3866	4.1949
		Present^a ($\epsilon_{zz}=0$)	7.8432	5.7628	4.5793	7.6710	5.6018	4.4189	7.4904	5.4331	4.2505
		HSBT [3]	-	-	-	7.6651	5.5616	4.3962	-	-	-
	ΔC=2%	Present ($\epsilon_{zz}=0$)	8.1173	5.8659	4.5388	7.9368	5.6941	4.3623	7.7475	5.5137	4.1760
		Present ($\epsilon_{zz}\neq0$)	7.7835	5.6076	4.3164	7.5951	5.4273	4.1300	7.3970	5.2374	3.9323
		Present^a ($\epsilon_{zz}=0$)	7.7973	5.6348	4.3603	7.6240	5.4699	4.1908	7.4423	5.2967	4.0120
		HSBT [3]	-	-	-	-	-	-	7.4365	5.2518	3.9832
C-H	ΔC=0%	Present ($\epsilon_{zz}\neq0$)	12.3395	9.1845	7.4860	12.2043	9.0631	7.3697	12.0640	8.9374	7.2497
	ΔC=1%	Present ($\epsilon_{zz}\neq0$)	12.3027	9.0839	7.3194	12.1671	8.9609	7.1996	12.0263	8.8335	7.0759
	ΔC=2%	Present ($\epsilon_{zz}\neq0$)	12.2659	8.9822	7.1486	12.1298	8.8574	7.0250	11.9885	8.7282	6.8974
C-C	ΔC=0%	Present ($\epsilon_{zz}\neq0$)	17.8621	13.2929	10.8379	17.7660	13.2106	10.7608	17.6668	13.1258	10.6817
	ΔC=1%	Present ($\epsilon_{zz}\neq0$)	17.8352	13.2192	10.7164	17.7389	13.1363	10.6379	17.6395	13.0509	10.5573
	ΔC=2%	Present ($\epsilon_{zz}\neq0$)	17.8082	13.1452	10.5933	17.7118	13.0616	10.5133	17.6122	12.9755	10.4313

^{a}: $Q_{11} = E(z)$

Table 13: Fundamental frequency ($\hat{\omega}$) of Si$_3$N$_4$/SUS304 beams under sinusoidal moisture and temperature rise(L/h=20, TD).

| BCs	ΔC	Theory	ΔT=0			ΔT=20			ΔT=40		
			p=0.2	1	5	p=0.2	1	5	p=0.2	1	5
H-H	ΔC=0%	Present ($\epsilon_{zz}=0$)	8.2127	6.1295	4.9846	8.0857	6.0152	4.8730	7.9533	5.8962	4.7572
		Present ($\epsilon_{zz}\neq 0$)	7.8828	5.8824	4.7825	7.7504	5.7629	4.6656	7.6122	5.6383	4.5440
		Present^a ($\epsilon_{zz}=0$)	7.8889	5.8879	4.7882	7.7670	5.7781	4.6811	7.6399	5.6639	4.5699
		HSBT [3]	7.8817	5.8491	4.7664	-	-	-	-	-	-
	ΔC=1%	Present ($\epsilon_{zz}=0$)	8.1874	6.0529	4.8399	8.0600	5.9370	4.7244	7.9272	5.8163	4.6044
		Present ($\epsilon_{zz}\neq 0$)	7.8565	5.8026	4.6316	7.7236	5.6813	4.5104	7.5848	5.5547	4.3841
		Present^a ($\epsilon_{zz}=0$)	7.8646	5.8143	4.6493	7.7423	5.7030	4.5385	7.6148	5.5872	4.4232
		HSBT [3]	-	-	-	7.7355	5.6625	4.5149	-	-	-
	ΔC=2%	Present ($\epsilon_{zz}=0$)	8.1619	5.9753	4.6907	8.0341	5.8577	4.5710	7.9009	5.7353	4.4464
		Present ($\epsilon_{zz}\neq 0$)	7.8300	5.7217	4.4757	7.6967	5.5985	4.3496	7.5574	5.4699	4.2180
		Present^a ($\epsilon_{zz}=0$)	7.8402	5.7398	4.5061	7.7175	5.6270	4.3912	7.5896	5.5094	4.2716
		HSBT [3]	-	-	-	-	-	-	7.5826	5.4650	4.2429
C-H	ΔC=0%	Present ($\epsilon_{zz}\neq 0$)	12.3395	9.1845	7.4860	12.2436	9.1010	7.4057	12.1444	9.0147	7.3230
	ΔC=1%	Present ($\epsilon_{zz}\neq 0$)	12.3199	9.1253	7.3749	12.2239	9.0411	7.2928	12.1245	8.9540	7.2085
	ΔC=2%	Present ($\epsilon_{zz}\neq 0$)	12.3003	9.0656	7.2619	12.2041	8.9807	7.1781	12.1045	8.8930	7.0919
C-C	ΔC=0%	Present ($\epsilon_{zz}\neq 0$)	17.8621	13.2929	10.8379	17.7948	13.2382	10.7870	17.7252	13.1818	10.7347
	ΔC=1%	Present ($\epsilon_{zz}\neq 0$)	17.8478	13.2495	10.7567	17.7804	13.1946	10.7051	17.7107	13.1379	10.6521
	ΔC=2%	Present ($\epsilon_{zz}\neq 0$)	17.8334	13.2059	10.6748	17.7659	13.1507	10.6225	17.6962	13.0938	10.5687

^{a}: $Q_{11} = E(z)$
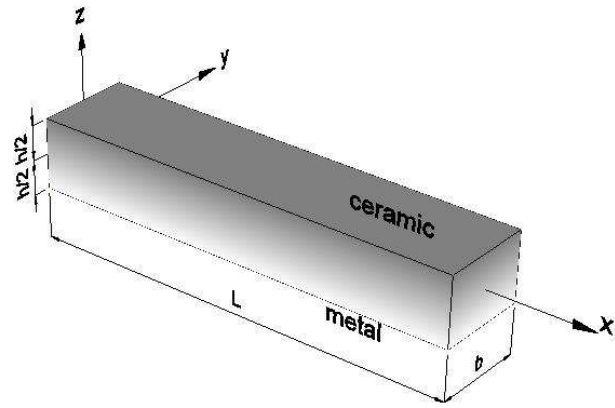
(a)
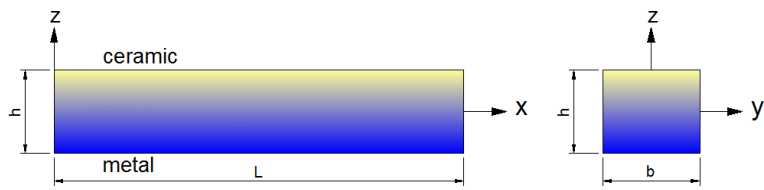
(b)
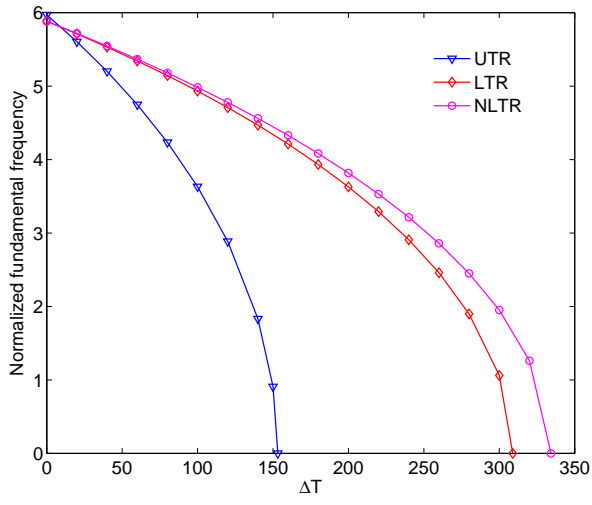
Figure 1: Geometry of FG beams.
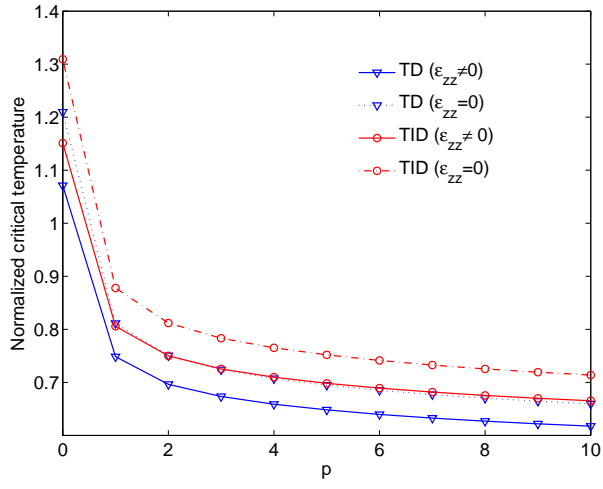
(a) λ of Si$_3$N$_4$/SUS304 beams with L/h=20
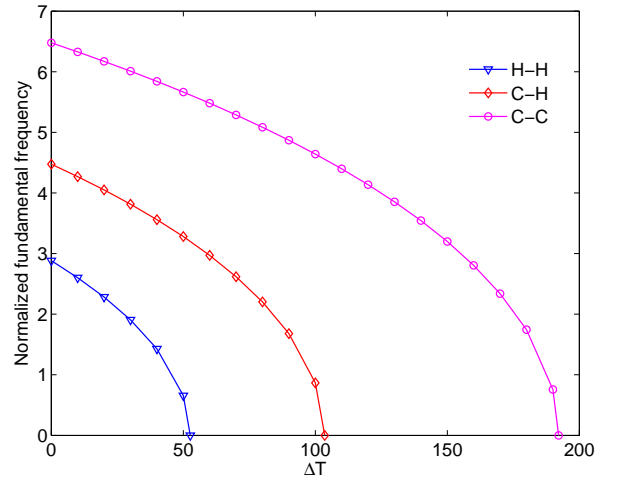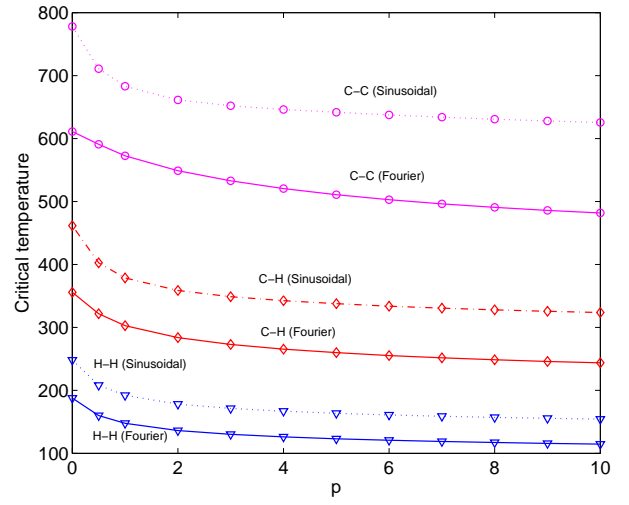
(b) $\bar{\omega}$ of Al$_2$O$_3$/SUS304 beams with L/h=30 and p=2

Figure 2: Variation of normalized critical temperature and fundamental frequency of FG beams with respect to the power-law index p and uniform temperature rise ΔT.
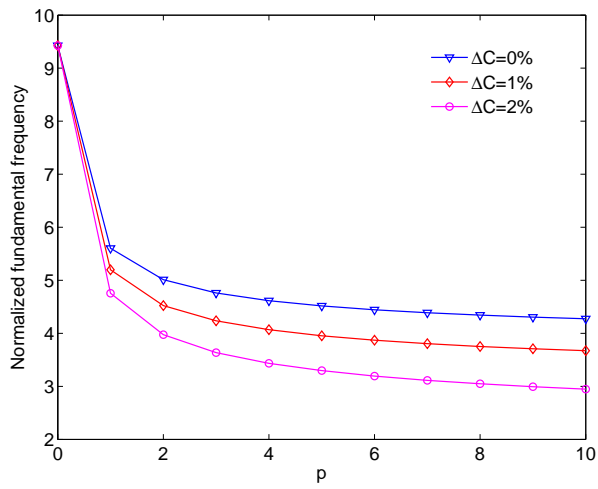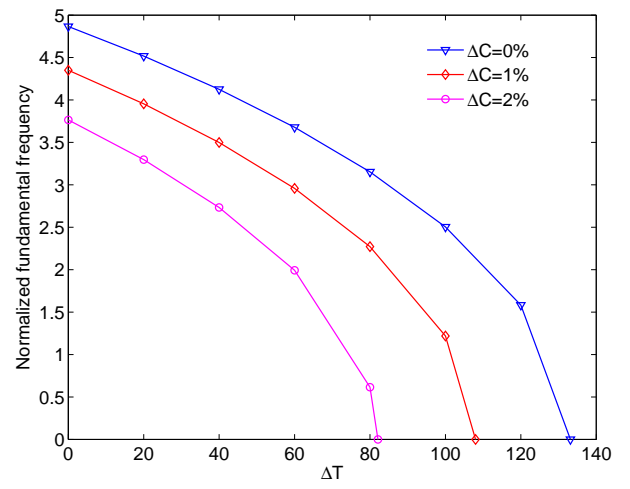
(a) $p = 1$ and L/h=20

(b) L/h=30

Figure 3: Variation of normalized fundamental frequency of Si_3N_4/SUS304 beams with respect to the power-law index p and temperature rise (TD).

(a) $\Delta T=20$ (b) $p = 5$

Figure 4: Variation of normalized fundamental frequency of Si_3N_4/SUS304 beams with respect to the power-law index, moisture and temperature rise (L/h=20, TD).